Influences of Large-scale Smart Charging Stations on Small-Signal Stability of Power Systems

Cai, H., Huang, J., Wang, H., Xie, Z., Chen, Q., & Littler, T. (2014). Influences of Large-scale Smart Charging Stations on Small-Signal Stability of Power Systems. Proceedings of the CSEE, 34(16), 2561-2574. DOI: 10.13334/j.0258-8013.pcsee.2014.16.006

Published in:
Proceedings of the CSEE

Document Version:
Version created as part of publication process; publisher's layout; not normally made publicly available

Queen's University Belfast - Research Portal:
Link to publication record in Queen's University Belfast Research Portal

DOI：10.13334/j.0258-8013.pcsee.2014.16.006 文章编号：0258-8013 (2014) 16-2561-13 中图分类号：TM 71

大规模电动汽车智能充电站对电力系统小干扰稳定性的影响

蔡晖[1]，黄俊辉[1]，王海潜[1]，谢珍建[1]，陈麒宇[2]，Tim LITTLER[2]

(1. 国网江苏省电力公司经济技术研究院，江苏省 南京市 210009;
2. 贝尔法斯特女王大学，英国 贝尔法斯特 BT9 5AH)

Influences of Large-scale Smart Charging Stations on Small-Signal Stability of Power Systems

CAI Hui[1], HUANG Junhui[1], WANG Haiqian[1], XIE Zhenjian[1], CHEN Qiyu[2], Tim LITTLER[2]

(1. State Grid Jiangsu Economic Research Institute, Nanjing 210009, Jiangsu Province, China; 2. School of Electronics, Electrical Engineering and Computer Science, Queen's University Belfast, Belfast BT9 5AH, United Kingdom)

ABSTRACT: Large-scale smart charging stations can effectively satisfy and control the charging demands of tremendous plug-in electric vehicles (PEVs). But simultaneously their penetrations inevitably induce new challenges to the operation of power systems. In this paper, damping torque analysis (DTA) was employed to examine the effects of the integration of smart charging station on the dynamic stability of the transmission system. While the discussion has focused on the damping of power system oscillations in the transmission system, and the smart charging station in the distribution system can be considered as an equivalent one with the proper control connecting to the specified bus. A single-machine infinite-bus power system with a smart charging station which denoted the equivalent of several ones was used for analysis. From the results obtained from DTA, it reveals that in the view of the damping ratio, the optimal charging capacity is better to be considered in the design of the smart charging station. Under the proposed charging capacity, the power system can achieve the best maintained dynamic stability, and the damping ratio can reach the crest value. According to the established Phillips-Heffron model in the previous analysis, the phase compensation method was utilized to design the stabilizer via the active and reactive power regulators of the smart charging station respectively. With the help of the stabilizers, damping of the system oscillation under certain operating conditions can be significantly improved, and the power oscillation in the tie-line can be suppressed more quickly. The results of the case study verified the conclusions.

KEY WORDS: smart charging station; plug-in electric vehicles (PEVs); power system oscillations; small-signal stability; damping torque analysis (DTA); stabilizer design

摘要：大规模智能充电站可以很好地满足和调节电动汽车的充电需求，但同时也不可避免地给电网的稳定性运行带来新的影响和挑战。基于阻尼转矩分析法(damping torque analysis，DTA)，着重探讨智能充电站的接入对于输电网动态稳定性的影响。为了简化分析，单机无穷大系统将用于模拟配电网与外部输电网。配电网中的智能充电站群被视为一个接入输电网的等值智能充电站。分析得出，在大规模智能充电站的设计中，充电容量对于小干扰稳定性中的阻尼比有很大的影响。在其最佳充电容量下充电，将会最有利于保持系统的动态稳定，系统阻尼比也保持最大。根据所建立的 Phillips-Heffron 模型可知，在智能充电站的有功和无功控制通道上设计并加装稳定器，能够有效地提高系统阻尼，更快地抑制联络线上的功率振荡。算例分析验证了所得结论。

关键词：智能充电站；电动汽车；功率振荡；小干扰稳定性；阻尼转矩分析法；稳定器设计

0 INTRODUCTION

The growing concern of carbon dioxide emission, greenhouse effect and rapid depletion of fossil energy drives the demand for the revolutionary changes in the automobile industry. Much effort has been put into developing a new high-efficient, environment-friendly and safe transportation vehicle that can replace the conventional ones. The utilization of plug-in electric vehicles (PEVs) as the most suitable solution has been promoted in many countries. China is expected to

have 5 million EVs by 2020 according to its Development Plan for Energy-saving and Renewable Energy Vehicles. However, a prediction by State Grid Corporation of China (SGCC) illustrates that the number will be 5 to 10 million due to fast development of EVs at present in China. As EV related technologies have been making progress and many national and local incentives have been created for EVs purchases, the total number of EVs is likely to be 30 million by 2030 [1-2].

With the significant increase of PEVs, the corresponding parking lots termed as smart charging stations in [3-5] will be established to charge the tremendous PEVs. A typical city will contain several SmartParks distributed throughout the city one to few miles apart in the distribution system. The newly established smart charging stations are preferred to be connected to an additional bus of the transmission system[3-5]. Vehicle-to-grid (V2G) technology supplies the bidirectional communication between the parked vehicles and connected grid. The vehicles parked in the smart charging station can not only simply absorb active power from the grid for charging, but also participate in power regulation during discharging mode. Reference [6] showed that most personal vehicles in the U.S. were parked more than 95% of the day and generally followed a daily schedule. The huge number of parked PEVs has the assignable potential to impact the frequency stability, voltage stability and rotor-angle stability of the system[7-12]. Nowadays, the capacity of smart charging stations is much lower than that of the conventional power plants. Only frequency stability and voltage stability of the distribution systems attract much attention in recent years. However, if only half of the 230 million gasoline-powered cars, sport utility vehicles and light trucks in U.S. are converted to or replaced with the electric vehicles, they would have 20 times the power capacity of all electricity in the country [13]. The impacts of SmartParks to the stability of the transmission systems cannot be ignored any more. Power system oscillations, as one section of the dynamic stability, occur inherently due to the rotor inertia of synchronous generators such that it takes time for them to respond to the sudden lack or excess of active power in a power system. The increased- amplitude or weak-damped power oscillations via the tie-lines will lead to the wrong activation of the automatic protection devices, the splitting of the system or even the collapse. While the time-varying of the load-flow condition in the power system with high-penetrated smart charging stations is the common reason for the appearance of power oscillations, damping torque of the system needs to be extremely concerned.

Under different operating conditions, smart charging stations can vary from the adjustable load in the charging mode to the regulable generator in the discharging mode and vice versa with the voltage control strategy[3-5]. It is significantly valuable to examine how and why it may interact with the conventional power generation, hence affecting power system small-signal stability. In order to gain a good understanding on and clear insight into this interaction through theoretical analysis, a single-machine infinite-bus power system is adopted in this paper. A smart charging station is connected to the system and theoretical damping torque analysis is carried out to check how and why the smart charging station interacts with the single generator so as to affect the power oscillation. It is expected that the analytical conclusions obtained in the paper can be used to guide further work on a more complicated case of the oscillations in multi-machine power systems.

The organization of this paper is as follows: in Section 1, a comprehensive model of a single-machine infinite-bus power system integrated with a smart charging station is established. After that, damping torque analysis (DTA)[14-16] is employed to examine the effect of joint operation of a smart charging station and a conventional synchronous machine on system small-signal stability in Section 2. The result of the damping torque analysis indicates that the smart charging station does not contribute an extra mode of electromechanical oscillation. It affects power system small-signal stability by supplying either positive or negative damping torque to the conventional power plant varying with the system operating conditions.

Analysis also reveals that from the view of damping ratio, the optimal charging capacity is better to be considered during the design of the smart charging station. In Section 3, the phase compensation method is utilized to design the stabilizer via the active and reactive power regulators of the smart charging station respectively. A single-machine infinite-bus power system integrated with a smart charging station is presented as an example in Section 4. Results of numerical computation, non-linear simulations and eigenvalue calculations at different system operating conditions are given. These simulations and results demonstrate and confirm the presented theoretical analysis, and verify the effectiveness of the designed stabilizer. Another 4-machine power system is employed to manifest that the conclusions obtained in the single-machine power system are also available in the multi-machine power system. Conclusions are summarized in Section 5.

1　A LINEARIZED MODEL OF SINGLE-MACHINE INFINITE-BUS SYSTEM WITH A SMART CHARGING STATION

The local electricity generations, except supporting the regional loads, can be used to charge a smart charging station under usual conditions. Comparing with thousand-million-kilowatt capacity of outer power systems, the abundant active power generation with ten-thousand-kilowatt capacity in a regional system can be simplified as an equivalent synchronous machine. The inertia of the equivalent synchronous machine denotes the dynamic stability of the regional system. Because every individual smart charging station has the same dynamic behavior during the transient procedure, the smart charging stations can be regarded as an equivalent one with higher active power and reactive power capacities. A smart charging station usually is connected to the transmission system through a step-up transformer, which is seemed as a reactance in this paper.

In this paper, the research focuses on the power oscillation which lasts for mostly ten to twenty seconds. Uncertainties during EV charging such as the alternations of charging strategies or vehicle numbers have little effect on this analysis. EV charging demand or discharging supply during this dynamic procedure is considered as determinate power from the start time and following seconds. For a simple analysis, a constant power charging/discharging strategy is utilized to estimate the optimal EV charging numbers for smart charging station design.

Fig. 1 shows the configuration of a single-machine infinite-bus power system, where a smart charging station is connected at a busbar denoted by subscript s. The linearized models of network equations and synchronous machine are presented in [14, 17-18].

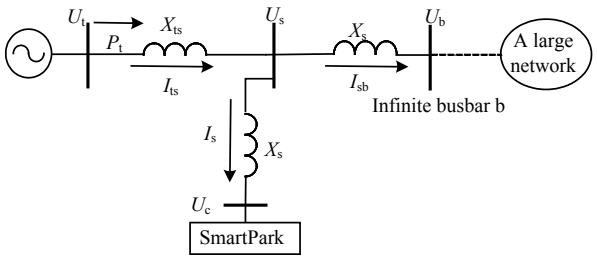

图 1　智能充电站接入单机无穷大电网

Fig. 1　Simplified model of the power system in a city

Where U_s is the voltage at the high-voltage-level busbar where the smart charging station locates; U_b, U_c are the voltages at infinite busbar and the low-voltage-level busbar connected with the smart charging station; I_{ts}, I_s, I_{sb} are the line currents as indicated in Fig. 1; X_{ts}, X_{sb}, X_s are line reactances as indicated in Fig. 1

The control strategy of smart charging stations is shown in Fig. 2. The objective control is to command the currents corresponding to the fast change in demanded active and reactive power. The equations of smart charging stations according to Fig. 2 are obtained as:

$$\begin{cases} P_1 = (K_{\mathrm{PP}} + K_{\mathrm{IP}}/s)(P_{\mathrm{PEVref}} - P_{\mathrm{PEV}}) \\ I_{q\mathrm{sref}} = \dfrac{P_1 + P_{10}}{U_s} \\ U_{q\mathrm{c}1} = (K_{\mathrm{PI}_q} + K_{\mathrm{II}_q}/s)(I_{q\mathrm{sref}} - I_{qs}) \\ U_{q\mathrm{c}} = U_{q\mathrm{c}0} + U_{q\mathrm{c}1} \\ Q_1 = (K_{\mathrm{PQ}} + K_{\mathrm{IQ}}/s)(Q_{\mathrm{PEVref}} - Q_{\mathrm{PEV}}) \\ I_{d\mathrm{sref}} = \dfrac{Q_1 + Q_{10}}{U_s} \\ U_{d\mathrm{c}1} = (K_{\mathrm{PI}_d} + K_{\mathrm{II}_d}/s)(I_{d\mathrm{sref}} - I_{ds}) \\ U_{d\mathrm{c}} = U_{d\mathrm{c}0} + U_{d\mathrm{c}1} \end{cases} \tag{1}$$

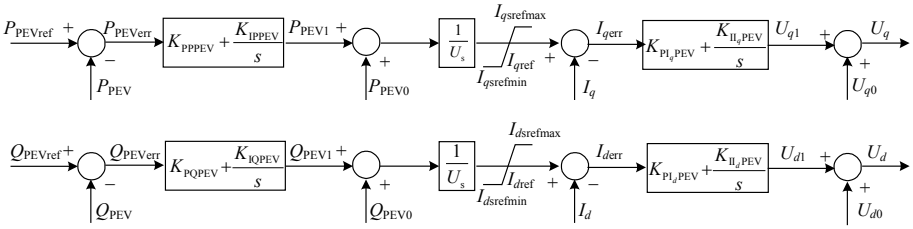

图 2 智能充电站控制框图

Fig. 2 Control strategy of a smart charging station

where

P_{PEV}, Q_{PEV} - the demanded active and reactive power by the smart charging station

$K_{\mathrm{PP}}+\frac{K_{\mathrm{IP}}}{s}, K_{\mathrm{PQ}}+\frac{K_{\mathrm{IQ}}}{s}, K_{\mathrm{PI}_d}+\frac{K_{\mathrm{II}_d}}{s}, K_{\mathrm{PI}_q}+\frac{K_{\mathrm{II}_q}}{s}$ are the Proportional-Integral controllers in the smart charging station.

Linearized from Equation (1),

$$\begin{cases}\Delta U_{d\mathrm{c}}=K_{\mathrm{U}_{dc}\mathrm{U}_{dc}}\Delta U_{d\mathrm{c}}+K_{\mathrm{U}_{dc}\mathrm{U}_{qc}}\Delta U_{q\mathrm{c}}+\\ \qquad K_{\mathrm{U}_{dc}\mathrm{E}'_q}\Delta E'_q+K_{\mathrm{U}_{dc}\delta}\Delta\delta\\ \Delta U_{q\mathrm{c}}=K_{\mathrm{U}_{qc}\mathrm{U}_{dc}}\Delta U_{d\mathrm{c}}+K_{\mathrm{U}_{qc}\mathrm{U}_{qc}}\Delta U_{q\mathrm{c}}+\\ \qquad K_{\mathrm{U}_{qc}\mathrm{E}'_q}\Delta E'_q+K_{\mathrm{U}_{qc}\delta}\Delta\delta\end{cases}\tag{2}$$

where

$$\begin{cases}\Delta P_{\mathrm{PEV}}=K_{\mathrm{PPU}_{dc}}\Delta U_{d\mathrm{c}}+K_{\mathrm{PPU}_{qc}}\Delta U_{qc}+\\ \qquad K_{\mathrm{PPE}'_q}\Delta E'_q+K_{\mathrm{PP}\delta}\Delta\delta\\ \Delta Q_{\mathrm{PEV}}=K_{\mathrm{QPU}_{dc}}\Delta U_{d\mathrm{c}}+K_{\mathrm{QPU}_{qc}}\Delta U_{q\mathrm{c}}+\\ \qquad K_{\mathrm{QPE}'_q}\Delta E'_q+K_{\mathrm{QP}\delta}\Delta\delta\\ \Delta U_{\mathrm{s}}=K_{\mathrm{U_sU}_{dc}}\Delta U_{d\mathrm{c}}+K_{\mathrm{U_sU}_{qc}}\Delta U_{q\mathrm{c}}+\\ \qquad K_{\mathrm{U_sE}'_q}\Delta E'_q+K_{\mathrm{U_s}\delta}\Delta\delta\end{cases}\tag{3}$$

$$\Delta T_{\mathrm{et\text{-}ex}}=\Delta T_{\mathrm{st\text{-}ex}}+j\Delta T_{\mathrm{dt\text{-}ex}}=K_{\mathrm{PE}'_q}$$

$$\frac{-[K_{\mathrm{E}_q\mathrm{U}_{qc}}K_{\mathrm{sp\text{-}U}_{qc}\delta}+K_{\mathrm{E}_q\delta}-\frac{K_{\mathrm{a}}}{1+sT_{\mathrm{a}}}(K_{\mathrm{U_tU}_{dc}}K_{\mathrm{sp\text{-}U}_{dc}\delta}+K_{\mathrm{U_tU}_{qc}}K_{\mathrm{sp\text{-}U}_{qc}\delta}+K_{\mathrm{U_t}\delta})]}{(T'_{d0}s+K_{\mathrm{E}_q\mathrm{E}'_q})+K_{\mathrm{E}_q\mathrm{U}_{qc}}K_{\mathrm{sp\text{-}U}_{qc}\mathrm{E}'_q}-\frac{K_{\mathrm{a}}}{1+sT_{\mathrm{a}}}(K_{\mathrm{U_tU}_{dc}}K_{\mathrm{sp\text{-}U}_{dc}\mathrm{E}'_q}+K_{\mathrm{U_tU}_{qc}}K_{\mathrm{sp\text{-}U}_{qc}\mathrm{E}'_q}+K_{\mathrm{U_tE}'_q})}\Delta\delta\tag{6}$$

$$\Delta T_{\mathrm{et}}=\Delta T_{\mathrm{st}}+j\Delta T_{\mathrm{dt}}=\Delta T_{\mathrm{et\text{-}sp}}+\Delta T_{\mathrm{et\text{-}ex}}=(\Delta T_{\mathrm{st\text{-}sp}}+\Delta T_{\mathrm{st\text{-}ex}})+j(\Delta T_{\mathrm{dt\text{-}sp}}+\Delta T_{\mathrm{dt\text{-}ex}})\tag{7}$$

Fig.3 and Fig.4 clearly show the dynamic interaction between the smart charging station and the conventional synchronous generator. Fig. 3 is very similar to the conventional Phillips-Heffron model based on which the DTA was proposed and developed. It shows that the smart charging station interacts closely with the generator by contributing the electric torque to the electromechanical oscillation loop of the

Arranging from Equation (2),

$$\begin{cases}\Delta U_{d\mathrm{c}}=K_{\mathrm{sp\text{-}U}_{dc}\mathrm{E}'_q}\Delta E'_q+K_{\mathrm{sp\text{-}U}_{dc}\delta}\Delta\delta\\ \Delta U_{q\mathrm{c}}=K_{\mathrm{sp\text{-}U}_{qc}\mathrm{E}'_q}\Delta E'_q+K_{\mathrm{sp\text{-}U}_{qc}\delta}\Delta\delta\end{cases}\tag{4}$$

While this paper focuses on the analysis of the impact from the grid-connected smart charging station to the system small-signal stability, linearized processes and expressions for coefficients are not specifically listed.

2 Analysis of Damping Torque Contribution from Phillips-Heffron model

The Phillips-Heffron model of the single-machine infinite-busbar power system with a smart charging station can be obtained as Fig.3. From Equations (2) and (3), the

model of the smart charging station and its control strategy can be obtained as Fig. 4.

From Fig.3 and Fig.4, we have:

$$\Delta T_{\mathrm{et\text{-}sp}}=\Delta T_{\mathrm{st\text{-}sp}}+j\Delta T_{\mathrm{dt\text{-}sp}}=K_{\mathrm{PU}_{dc}}\Delta U_{d\mathrm{c}}+K_{\mathrm{PU}_{qc}}\Delta U_{q\mathrm{c}}=(K_{\mathrm{PU}_{dc}}K_{\mathrm{sp\text{-}U}_{dc}\delta}+K_{\mathrm{PU}_{qc}}K_{\mathrm{sp\text{-}U}_{qc}\delta})\Delta\delta\tag{5}$$

generator. The contribution of electric torque is comprised by two parts, i.e. $\Delta T_{\mathrm{et\text{-}sp}}$ which relates to $\Delta\delta$ and directly affects the oscillation loop, and $\Delta T_{\mathrm{et\text{-}ex}}$ which relates to $\Delta E'_q$ and functions through the excitation system, as indicated in Fig. 3. According to DTA, the electric torque can be decomposed into two components, i.e. the synchronizing torque and the damping torque as shown in Equation (7). The damping torque contributions $\Delta T_{\mathrm{dt\text{-}sp}}$, $\Delta T_{\mathrm{dt\text{-}ex}}$ and ΔT_{dt} determine the influences on the damping of power

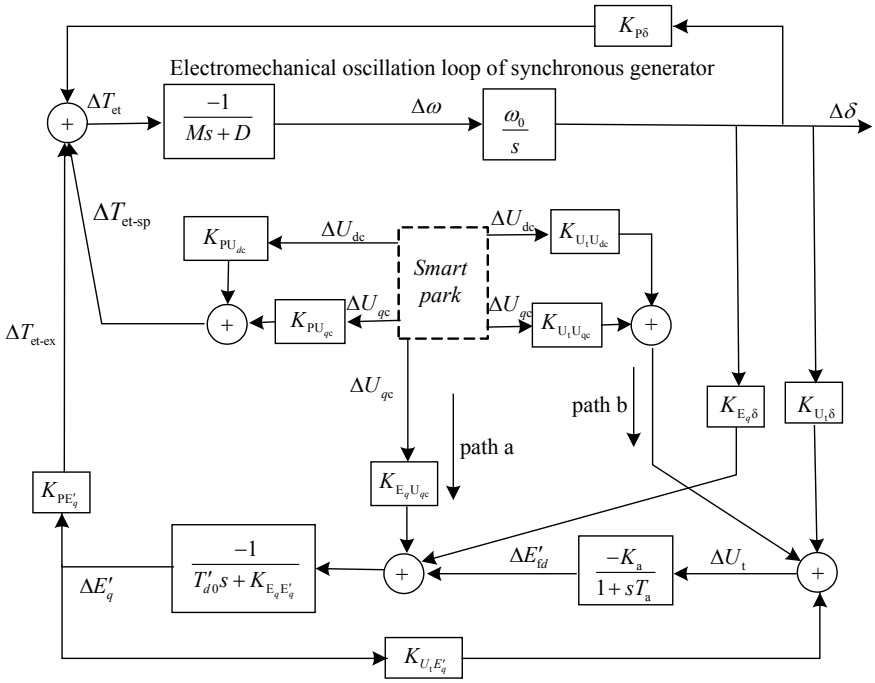

图 3　智能充电站接入单机无穷大系统的 Phillips-Heffron 模型

Fig. 3　Phillips-Heffron model of the single-machine infinite-busbar system with a smart charging station

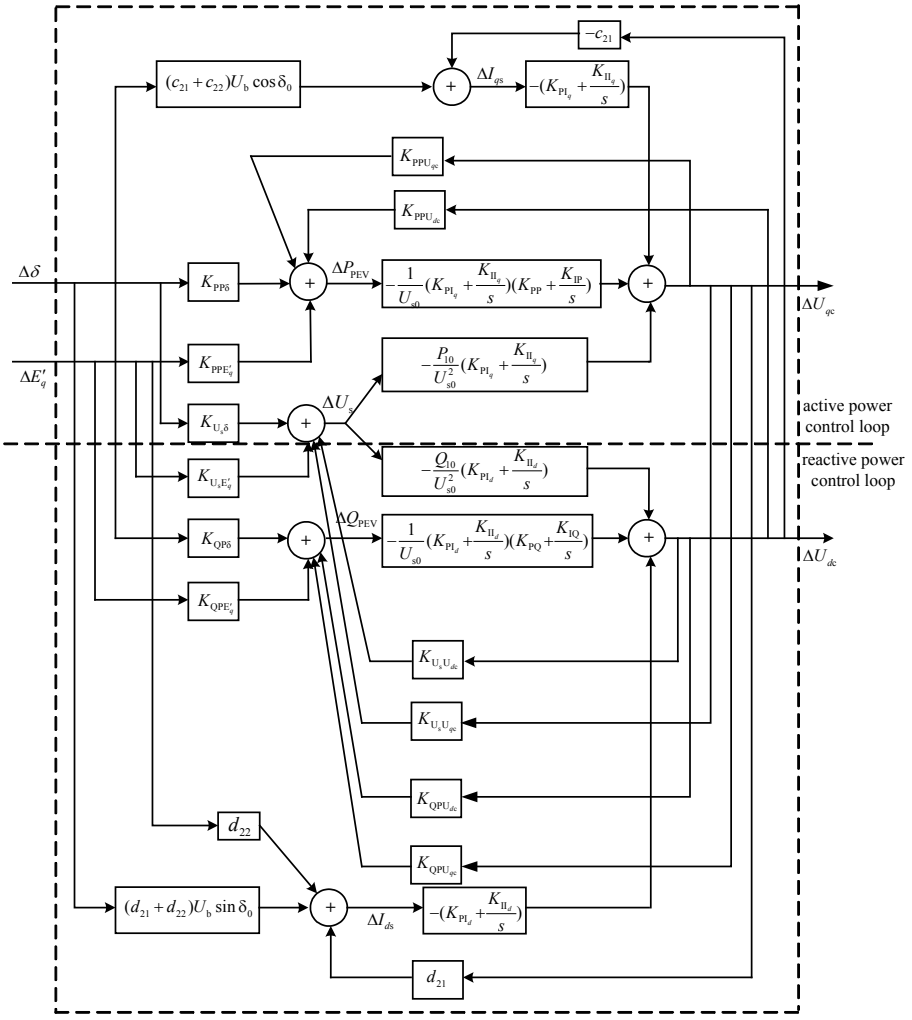

图 4　智能充电站控制器的线性化模型

Fig. 4　Linearized model of a smart charging station and its control

system oscillation.

With certain output power of the synchronous machine and absorbed or injected power of the smart charging station, the bus voltages and currents of the corresponding operation condition can be determined. The damping torques $\Delta T_{\text{dt-sp}}$, $\Delta T_{\text{dt-ex}}$ and ΔT_{dt} are dependent on the output power of the synchronous machine and the absorbed or injected power of the smart charging station.

From Equations (5)-(7), the conclusions can be summarized as follows:

1）The proportional controls K_{p} in the smart charging station mainly induce the synchronous torque into the oscillation loop, while for $\Delta T_{\text{et-sp}}$ in Equation (5), only its real part is related to $\Delta\delta$, and the majority of damping torque is introduced by integral controls K_{i}/s, because $1/s$ induces the image part in $\Delta T_{\text{et-sp}}$ relating to $\Delta\omega$.

2）Because the signals ΔU_{dc} and ΔU_{qc} through path a and path b in Fig. 3 are significantly attenuated by lag loops before they form one part of the damping torque through the excitation system[19], the damping torque contribution from them can be neglected for simplified analysis. $\Delta T_{\text{dt-sp}}$ represents the main damping torque supplied by the smart charging station in damping torque analysis, and $\Delta T_{\text{dt-ex}}$ mainly expresses the torque supplied by the excitation system of the synchronous machine.

3）In this paper, '–' sign indicates the vehicles are selling power to the grid, that is, they are in discharging mode and '+' sign indicates that they are buying power from the gird, denoting that the vehicles are in charging mode.

The optimal operation point when the system has the biggest damping torque can be calculated as:

$$\frac{\partial \Delta T_{\text{dt}}}{\partial P_{\text{PEV}}}=\frac{\partial \Delta T_{\text{dt-sp}}+\partial \Delta T_{\text{dt-ex}}}{\partial P_{\text{PEV}}}=0 \,\&\, \frac{\partial^2 \Delta T_{\text{dt}}}{\partial P_{\text{PEV}}^2}\le 0,$$

$$P_{\text{PEV}}>0 \tag{8}$$

When the output power of the synchronous machine is fixed, the positive or negative damping torque supplied by the excitation system of the synchronous machine is only slightly changed. At the optimal operation point, the total damping torque ΔT_{dt} of the system and $\Delta T_{\text{dt-sp}}$ contributed from the smart charging station both reach to their maximum values.

When the active power in the tie-line is fixed, the output power of the synchronous machine is changed corresponding to the absorbed or injected power of the smart charging station. Both damping torques contributed by the smart charging station and the excitation system need to be considered. The total damping torque ΔT_{dt} of the system and $\Delta T_{\text{dt-sp}}$ contributed from the smart charging station reach to their maximum values at different operation points.

3 DESIGN FOR THE STABILIZER ATTACHED TO THE SMART CHARGING STATION

Under the operation conditions that the total damping torques supplied by the smart charging station and the excitation system are not enough to suppress the oscillations, the additional damping torques need to be added. Compared with the installation and coordinated parameter setting for power system stabilizers (PSSs) in synchronous machines, smart charging stations can be simply utilized to suppress the grid's active power oscillation with little infrastructure cost. Only a centralized stabilizer will be required at the smart charging station to maintain system stability.

The stabilizer added via the active power (AP) or reactive power (RP) control loop is shown in Fig. 5.

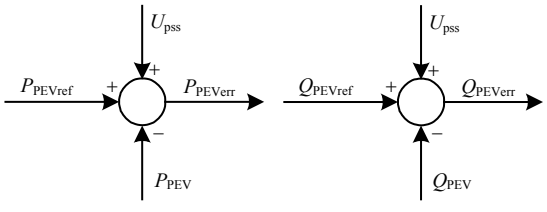

图 5 接入智能充电站有功及无功通道的稳定器控制策略

Fig. 5 Control strategy of the stabilizer added via AP and RP control loop respectively

The forward path function which describes the way from output signal of the stabilizer to the additional damping torque into the electromechanical oscillation loop can be obtained:

$$\begin{cases} F_{\text{pssp}}(s)=\dfrac{\partial \Delta T_{\text{pss}}}{\partial \Delta u_{\text{pssp}}}=K_{\text{PU}_{dc}}K_{\text{sp-U}_{dc}\text{u}_{\text{pssp}}}+K_{\text{PU}_{qc}}K_{\text{sp-U}_{qc}\text{u}_{\text{pssp}}}+ \\ \qquad K_{\text{PE}'_q}\dfrac{-[K_{\text{E}_q\text{U}_{qc}}K_{\text{sp-U}_{qc}\text{u}_{\text{pssp}}}-\dfrac{K_{\text{a}}}{1+sT_{\text{a}}}(K_{\text{U}_{\text{t}}\text{U}_{dc}}K_{\text{sp-U}_{dc}\text{u}_{\text{pssp}}}+K_{\text{U}_{\text{t}}\text{U}_{qc}}K_{\text{sp-U}_{qc}\text{u}_{\text{pssp}}})]}{(T'_{d0}s+K_{\text{E}_q\text{E}'_q})+K_{\text{E}_q\text{U}_{qc}}K_{\text{sp-U}_{qc}\text{E}'_q}-\dfrac{K_{\text{a}}}{1+sT_{\text{a}}}(K_{\text{U}_{\text{t}}\text{U}_{dc}}K_{\text{sp-U}_{dc}\text{E}'_q}+K_{\text{U}_{\text{t}}\text{U}_{qc}}K_{\text{sp-U}_{qc}\text{E}'_q}+K_{\text{U}_{\text{t}}\text{E}'_q})} \\ F_{\text{pssq}}(s)=\dfrac{\partial \Delta T_{\text{pss}}}{\partial \Delta u_{\text{pssq}}}=K_{\text{PU}_{dc}}K_{\text{sp-U}_{dc}\text{u}_{\text{pssq}}}+K_{\text{PU}_{qc}}K_{\text{sp-U}_{qc}\text{u}_{\text{pssq}}}+K_{\text{PE}'_q} \\ \qquad \dfrac{-[K_{\text{E}_q\text{U}_{qc}}K_{\text{sp-U}_{qc}\text{u}_{\text{pssq}}}-\dfrac{K_{\text{a}}}{1+sT_{\text{a}}}(K_{\text{U}_{\text{t}}\text{U}_{dc}}K_{\text{sp-U}_{dc}\text{u}_{\text{pssq}}}+K_{\text{U}_{\text{t}}\text{U}_{qc}}K_{\text{sp-U}_{qc}\text{u}_{\text{pssq}}})]}{(T'_{d0}s+K_{\text{E}_q\text{E}'_q})+K_{\text{E}_q\text{U}_{qc}}K_{\text{sp-U}_{qc}\text{E}'_q}-\dfrac{K_{\text{a}}}{1+sT_{\text{a}}}(K_{\text{U}_{\text{t}}\text{U}_{dc}}K_{\text{sp-U}_{dc}\text{E}'_q}+K_{\text{U}_{\text{t}}\text{U}_{qc}}K_{\text{sp-U}_{qc}\text{E}'_q}+K_{\text{U}_{\text{t}}\text{E}'_q})} \end{cases} \tag{9}$$

where F_{pssp} or F_{pssq} is corresponding to the utilized output signal of the stabilizer u_{pssp} or u_{pssq}.

$K_{\text{sp-U}_{dc}\text{u}_{\text{pssp}}}$, $K_{\text{sp-U}_{qc}\text{u}_{\text{pssp}}}$, $K_{\text{sp-U}_{dc}\text{u}_{\text{pssq}}}$ and $K_{\text{sp-U}_{qc}\text{u}_{\text{pssq}}}$ are obtained from the linearization of the control strategy with the output signals of the stabilizer considered.

The active power P_{b} in the tie-line is chosen for the feedback signals of the stabilizers via the active power regulator and the reactive power regulator.

From the linear system control theory, the active power P_{b} can be written as the function of the rotor speed of the generator.

$$\Delta P_{\text{b}}=r_{\text{P}}(s)\Delta\omega \tag{10}$$

where

$r_{\text{P}}(s)=(K_{\text{P}_{\text{b}}\delta}+K_{\text{P}_{\text{b}}\text{E}'_q}K_{\text{E}'_q\delta})\dfrac{\omega_0}{s}$ is the reconstruction function for P_{b}.

While $\Delta P_{\text{b}}=\Delta P_{\text{t}}-\Delta P_{\text{PEV}}$, $K_{\text{P}_{\text{b}}\delta}$, $K_{\text{P}_{\text{b}}\text{E}'_q}$ and $K_{\text{E}'_q\delta}$ are related to the reconstruction of this feedback signal.

Considering Equations (9) and (10), the electric torques contributed by the stabilizer via active and reactive power regulators respectively are expressed as:

$$\begin{cases} \Delta \boldsymbol{T}(\Delta u_{\text{pssp}})=F_{\text{pssp}}(s)r_{\text{p}}(s)G_{\text{PEVP}}(s)\Delta\omega \\ \Delta \boldsymbol{T}(\Delta u_{\text{pssq}})=F_{\text{pssq}}(s)r_{\text{p}}(s)G_{\text{PEVQ}}(s)\Delta\omega \end{cases} \tag{11}$$

where $G_{\text{PEVP}}(s)$ and $G_{\text{PEVQ}}(s)$ are the transfer function of the stabilizer via active and reactive power regulators respectively.

The transfer function of the stabilizer is

$$G_{\text{PEV}}=K_{\text{w}}\frac{1+sT_2}{1+sT_1}\frac{1+sT_4}{1+sT_3} \tag{12}$$

The stabilizers are designed to compensate the lagging or leading angle of the forward path, in order to supply maximum positive damping into the system. The phase compensation method is used to design the parameters of the stabilizers.

4 CASE STUDY

4.1 Case Description

Two example cases are employed in this section. From Case A to Case D, a single-machine infinite-busbar power system is used. The parameters of the system are given in Appendix A 1）. Under different capacities of the smart charging station, computational results of the damping torque contribution from the smart charging station and the excitation system to the electromechanical oscillation loop of the single synchronous generator are obtained and confirmed by the eigenvalue of system oscillation mode. The critical point in which the system has the biggest damping torque is highlighted. In Case E, a 4-machine power system is presented. The parameters are given in Appendix A 2）. The eigenvalue related to the inter-area oscillation mode is concerned under different capacities of the smart charging station.

4.2 Case A: Utilizing Only Proportional Control in the Smart Charging Station and Fixing Load-flow in the Tie-line

With the load-flow in the tie-line fixed at 10MW, the comparison is done when only proportional control is utilized in the smart charging station under its different charging or discharging power capacities. The computational results of the example system are

shown in Tab. 1, when only P control is utilized in the smart charging station. From Tab. 1, it can be concluded that:

表 1 在智能充电站控制策略中仅使用比例控制环节时的阻尼计算结果

Tab. 1 Computational results of the example system when only P control is utilized in the smart charging station

P_t/ (10 MW)	P_{PEV}/ (10 MW)	ΔT_{dt}/ pu	$\Delta T_{dt\text{-}sp}$/ pu	$\Delta T_{dt\text{-}ex}$/ pu	Frequency/ Hz	Damping ratio/%
4.0	3.0	0.634 0	0.000 6	0.633 4	1.83	3.19
3.5	2.5	0.784 2	0.000 4	0.783 8	1.82	3.47
3.0	2.0	0.436 8	0.000 2	0.436 6	1.74	2.99
2.5	1.5	−0.187 7	−0.000 3	−0.187 4	1.68	1.92
2.0	1.0	−0.573 0	−0.000 5	−0.572 5	1.61	1.24
1.5	0.5	−0.187 0	−0.000 2	−0.186 8	1.68	1.92
1.0	0.0	0.434 5	0.000 3	0.434 2	1.74	2.99
0.5	−0.5	0.785 1	0.000 5	0.784 6	1.82	3.47
0.0	−1.0	0.634 8	0.000 7	0.634 1	1.83	3.19

1）The total damping torque contribution ΔT_{dt} is approximately equal to the damping torque from the excitation system $\Delta T_{dt\text{-}ex}$. The change of ΔT_{dt} is mainly induced by $\Delta T_{dt\text{-}ex}$ which is the impact from the excitation system of the synchronous machine under different output power. The smart charging station only with the proportional control functions as an adjustable load in charging mode or as a regulator generator in discharging mode.

2）Integral control in the smart charging station not only helps to reduce the steady-state error and accelerates the smart charging station to the steady operation point, but also supplies either positive or negative damping torque into the system. It demonstrates conclusion 1）obtained in Section 2.

4.3 Case B: Utilizing pi Control in the Smart Charging Station and Fixing Output Power Of The Synchronous Machine

The comparison of the damping torques is made under different charging or discharging power capacities of the smart charging station with the fixed output power of the synchronous machine. The computational results of the example system are shown in Tab. 2, when active power supplied by the synchronous machine is fixed at 10 MW. From Tab. 2, it can be concluded that:

表 2 在同步机出力固定在 10 MW 时的阻尼计算结果

Tab. 2 Computational results of the example system when active power supplied by the synchronous machine is fixed at 10 MW

P_t/ (10 MW)	P_{PEV}/ (10 MW)	ΔT_{dt}/ pu	$\Delta T_{dt\text{-}sp}$/ pu	$\Delta T_{dt\text{-}ex}$/ pu	Frequency/ Hz	Damping ratio/%
1.0	3.0	0.063 3	−0.318 2	0.381 5	1.69	2.38
1.0	2.5	0.156 0	−0.245 2	0.402 1	1.72	2.51
1.0	2.0	0.374 2	−0.045 7	0.419 9	1.74	2.88
1.0	1.5	0.840 0	0.379 8	0.460 2	1.75	3.71
1.0	1.0	1.067 7	0.580 6	0.487 1	1.76	4.10
1.0	0.5	0.818 0	0.369 9	0.448 1	1.75	3.67
1.0	0.0	0.352 3	−0.058 2	0.410 5	1.74	2.84
1.0	−0.5	0.139 8	−0.259 3	0.399 1	1.72	2.48
1.0	−1.0	0.022 7	−0.337 0	0.359 7	1.70	2.29

1）While the output of the synchronous machine is constant, the damping torque from the excitation system of the synchronous machine is nearly unchanged. The signals ΔU_{dc} and ΔU_{qc} through path a and path b only contribute slight changes to $\Delta T_{dt\text{-}ex}$. The variety of total damping torque contribution ΔT_{dt} is mainly induced from $\Delta T_{dt\text{-}sp}$ which comes from the smart charging station and directly affects the oscillation loop. It demonstrates conclusion 2） obtained in Section 2.

2）The damping torque from the smart charging station changes at its different charging or discharging capacity, which is either positive or negative. The smart charging station can help to improve the damping with certain charging capacity which is between the lower and upper threshold. In charging mode, the smart charging station is preferred to operate around 10 MW which is nearly the same as 10.4 MW calculated by Equation (8). The highest total damping torque and damping torque from the smart charging station are coincided at the same point. It demonstrates conclusion 3）obtained in Section 2. Under this operation point, the smart charging station just consumes the electricity generated by the equivalent synchronous machine. There is no active power exchange in the tie-line. Beyond or below this point, the damping ratio of the system will decrease because of the increase load burden in the tie-line either from the synchronous machine to the infinite bus or vice versa. Considering each vehicle can draw

±3.5 kW active power [20] and always around 60% personal vehicles in the parking lots need to be charged[21], roughly 5000 personal vehicles are optimal to be accepted in this equivalent smart charging station.

3）During the discharging process, the damping of the system intends to deteriorate with the increasing power injected from the smart charging station to grid.

4.4 Case C: Utilizing PI Control IN The Smart Charging Station and Fixing Load Flow In the Tie-line

The comparison of the damping torques is made under different charging or discharging power capacities of the smart charging station with the fixed load flow in the tie-line. The results are shown in Tab. 3.

表 3　在联络线上功率固定在 10 MW 时的阻尼计算结果

Tab. 3　Computational results of the example system when load flow in the tie-line is fixed at 10 MW

P_t/ (10 MW)	P_{PEV}/ (10 MW)	ΔT_{dt}/ pu	$\Delta T_{dt\text{-}sp}$/ pu	$\Delta T_{dt\text{-}ex}$/ pu	Frequency/ Hz	Damping ratio/%
4.0	3.0	0.314 4	−0.287 8	0.602 2	1.72	2.80
3.5	2.5	0.552 7	−0.212 2	0.764 9	1.72	3.24
3.0	2.0	0.390 2	−0.008 2	0.398 4	1.72	2.94
2.5	1.5	0.177 0	0.315 2	−0.138 2	1.73	2.53
2.0	1.0	0.009 3	0.529 4	−0.520 1	1.73	2.22
1.5	0.5	0.169 3	0.312 2	−0.142 9	1.73	2.52
1.0	0.0	0.352 3	−0.058 2	0.410 5	1.74	2.84
0.5	−0.5	0.506 2	−0.209 1	0.715 3	1.73	3.14
0.0	−1.0	0.297 1	−0.290 8	0.587 9	1.73	2.75

From Tab. 3, it can be concluded that:

1）The total damping torque contribution ΔT_{dt} is simultaneously influenced by $\Delta T_{dt\text{-}sp}$ which relates to $\Delta\delta$ and directly affects the oscillation loop, and $\Delta T_{dt\text{-}ex}$ which relates to $\Delta E'_q$ and functions through the excitation system.

2）The damping torque supplied from the smart charging station and the excitation system of the synchronous machine respectively is complementary during the charging process. Compared with Tab. 1, the positive damping torque supplied by the smart charging station helps the system to improve the low damping from 5 MW to 15 MW in charging mode of the smart charging station. This conclusion can be confirmed by the analysis from Equation (5) and (6). When the charging power of the smart charging station is between 0 MW and 30 MW, the product of $\Delta T_{dt\text{-}sp}$ and $\Delta T_{dt\text{-}ex}$ is negative.

3）The impact of the damping torque from the synchronous machine also needs to be considered. With this impact, the highest total damping torque and damping torque from the smart charging station are obtained at different points. In this case, the optimized operation point reaches to 25 MW which is nearly the same as 24.6 MW calculated by Equation (8). It demonstrates conclusion 3）in Section 2. Under the operating conditions that the absorbed power of the smart charging station varies from 20MW to 25MW, although the smart charging station supplies the negative damping torque into the grid, the total damping torque is still positive and keeps increasing with the compensation of the damping torque from the excitation system. The smart charging station at the optimal operation point is also charged by the electricity generated by the equivalent local synchronous machine.

4）The damping of the system intends to deteriorate with the increasing power injected from the smart charging station to the grid during the discharging process.

4.5 Case D: Stabilizer Design

While the operation condition for the smart charging station varies stochastically, the stabilizer is designed and attached to the smart charging station to supply additional damping torques into the system.

The stabilizer via the active and reactive power loops is designed respectively under the condition that the equivalent synchronous machine supplies 20 MW and the smart charging station consumes 10 MW active power. A three-phase short-circuit fault happens in Bus s at 0.5 s and lasts for 0.1 s.

The forward path is:

$$\begin{cases} F_{pssp}(s) = -6.875\ 1 + \mathrm{j}6.829\ 3 \\ F_{pssq}(s) = 1.752\ 0 + \mathrm{j}7.284\ 1 \end{cases}$$

The parameters of the designed stabilizer attached to active and reactive power regulators respectively are shown in Tab. 4.

With the designed stabilizer, the eigenvalue of the system with the smart charging station can be obtained as shown in Tab. 5.

表 4 稳定器设计参数

Tab. 4 Parameters of smart charging station-based stabilizers

Stabilizer	Parameters
Stabilizer via active power regulator	T_1=T_3=0.019 5; T_2=T_4=0.5; K_W=16.570 4
Stabilizer via reactive power regulator	T_1=T_3=0.081 0; T_2=T_4=0.5; K_W=12.628 9

表 5 在 P_{PEV}=10 MW, P_t=20 MW 工况下，加入稳定器前后特征根对比

Tab. 5 Eigenvalue of the oscillation mode without and with stabilizers under P_{PEV}=10 MW, P_t=20 MW

Without the stabilizer	−0.241 9+j10.864 4
With the stabilizer via active power regulator	−0.759 0+j10.816 9
With the stabilizer via reactive power regulator	−0.651 1+j10.847 1

The effectiveness of the designed stabilizers is verified by the time-domain simulation in Fig. 6 and eigenvalue calculation in Tab. 5. From Tab. 5 and Fig. 6, it can be seen that the designed stabilizer attached to the smart charging station can not only help to reduce the power fluctuations for PEV charging, but also suppress the power oscillation in the tie-line.

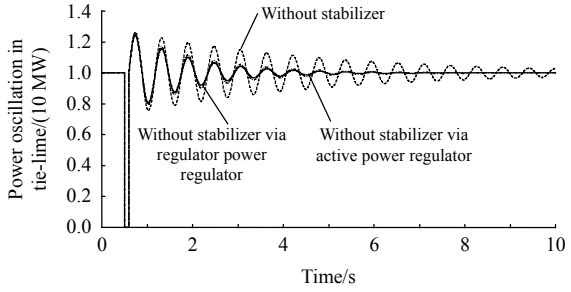

图 6 在 P_{PEV}=10 MW, P_t=20 MW 运行工况下，加入稳定器前后联络线上功率振荡的非线性仿真

Fig. 6 Comparisons of tie-line power oscillation without and with the stabilizer via active and reactive power regulators under P_{PEV}=10 MW, P_t=20 MW

4.6 Case E: Analysis in the 4-Machine Power System

The power system integrated with the smart charging station is shown in Fig. 7. Prony method is employed to analyze the time-domain simulation of the power flow in the tie-line $L_{6\text{-}7}$[22]. The critical inter-area electromechanical oscillation frequency $f_{critical}$ and its corresponding attenuation factor $\alpha_{critical}$ are extracted. The eigenvalue of the critical oscillation mode is $\lambda_{critical}=\alpha_{critical}+j2\pi f_{critical}$.

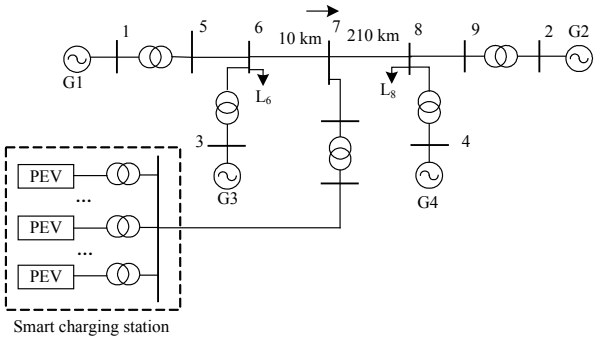

图 7 智能充电站接入 4 机 2 区域系统示意图

Fig. 7 Four-machine power system integrated with the smart charging station

With the load-flow in the tie-line $L_{6\text{-}7}$ fixed at 70 MW, the comparison is done between the proportional controlled smart charging station and the adjustable load/generator connected at Bus 7 respectively. The eigenvalue related to the inter-area oscillation mode is concerned. From Tab. 6, only the proportional controlled smart charging station functions as the adjustable load during charging period and as the regulable generator in discharging mode in the view of the damping ratio.

表 6 在智能充电站控制策略中仅使用比例控制环节时的阻尼计算结果

Tab. 6 Comparison of eigenvalue related to inter-area oscillation mode only utilizing the proportional control of the smart charging station

P_{G2}/(10 MW)	P_{PEV}/(10 MW)	Frequency/Hz	Damping ratio/%	Adjustable load/generator*/(10MW)	Frequency/Hz	Damping ratio/%
9.0	3.0	0.472 4	3.12	3.0	0.472 4	3.12
8.5	2.5	0.471 0	3.14	2.5	0.471 0	3.14
8.0	2.0	0.469 3	3.15	2.0	0.469 3	3.15
7.5	1.5	0.467 2	3.16	1.5	0.467 2	3.16
7.0	1.0	0.465 0	3.15	1.0	0.465 0	3.15
6.5	0.5	0.462 4	3.13	0.5	0.462 4	3.13
6.0	0.0	0.459 5	3.11	0.0	0.459 5	3.11
5.5	-0.5	0.456 4	3.07	-0.5	0.456 4	3.07
5.0	-1.0	0.453 0	3.01	-1.0	0.453 0	3.01

*:'+' denotes the adjustable load absorbing active power from the grid; '−' denotes the regulable generator injecting active power into the grid.

Proportional control of the smart charging station only supplies the synchronous torque and integral control that introduces the damping torque into the grid. Conclusion 1）obtained in the single-machine infinite-busbar power system is also available in the multi-machine power system.

Both proportional and integral controls are utilized in the smart charging station. The comparison is done under different charging or discharging power capacities of the smart charging station when the load-flow in the tie-line is fixed at 70 MW. The eigenvalue related to the inter-area oscillation mode is concerned. The results are shown in Tab. 7.

表 7　在智能充电站控制策略中使用比例积分控制环节时的阻尼计算结果

Tab. 7　Comparison of eigenvalue related to the inter-area oscillation mode utilizing PI control of the smart charging station

P_{G2}/(10 MW)	P_{PEV}/(10 MW)	Frequency/Hz	Damping ratio/%
9.0	3.0	0.473 4	2.52
8.5	2.5	0.477 8	2.64
8.0	2.0	0.480 2	2.98
7.5	1.5	0.475 3	2.56
7.0	1.0	0.472 5	2.48
6.5	0.5	0.468 3	2.34
6.0	0.0	0.461 1	2.25
5.5	−0.5	0.462 7	2.30
5.0	−1.0	0.472 1	2.39

From Tab. 7, the optimal charging point with the highest damping ratio in the single-machine power system can be obtained by Equation (8) and verified by the damping torque calculation; and it also exists in the multi-machine power system. But because of the complex interconnection of the synchronous machines and the smart charging station, it is difficult to calculate the optimal charging point in theory.

5　CONCLUSIONS

The paper investigates the impacts of a grid-connected smart charging station on power system small-signal stability based on a simple single-machine infinite-bus power system integrated with a smart charging station. Damping torque analysis (DTA) is employed to examine the contribution from the smart charging station to the electromechanical oscillation loop of the generator in theoretical analysis. The analysis has concluded that, the smart charging station affects power system small-signal stability in light of its interaction with the synchronous machine. The proportional controls in the smart charging station mainly induce the synchronous torque into the oscillation loop and the majority of damping torque is introduced by integral controls. The damping torque supplied by the smart charging station is mainly directly induced into the oscillation loop, and the damping torque from the excitation system is almost from the synchronous machine itself. The optimal operation condition of the smart charging station is the moment when the system has the highest damping ratio. In this paper, such an optimal operation condition is defined, indicating that the optimal charging capacity is considered for smart charging station design.

Results of the damping torque computation of a single-machine power system integrated with a smart charging station, confirmed by eigenvalue calculations of system oscillation mode, are presented in the paper. The conclusions obtained from the theoretical analysis are demonstrated and verified by these results. Under the optimal operation condition, the total damping torque supplied from the smart charging station and synchronous machine reaches its maximum value. During the discharging process, the damping of the system intends to deteriorate with the increasing power injected from the smart charging station to the grid. Another 4-machine power system is employed to manifest that the conclusions obtained in the single-machine power system are also available in the multi-machine power system.

The stabilizer is designed and attached to the active or reactive power regulator of the smart charging station to supply additional positive damping into the system. The phase compensation method is used here. The effectiveness is confirmed by the non-linear simulations and eigenvalue calculations in the single-machine power system.

Although the configuration of the power system with the grid-connected smart charging station and the

function to describe the charging/discharging behaviors of EVs adopted in this paper are very simple, all the essential elements have been included to serve the purpose of study, which can thoroughly reveal the dynamic interaction between the equivalent smart charging station and conventional generation in the transmission system. The optimal charging capacity is better to be considered during the capacity design of the smart charging station. With the help of the designed smart charging station-based stabilizer, the small-signal stability can be effectively maintained. Studies on the interactions among several smart charging stations to the dynamic stability in distribution systems and the uncertainties and diversities of EV charging/discharging behaviors will be carried out for future researches.

Acknowledgements

The authors would like to acknowledge the support of the science bridge award (EP/G042594/1).

REFERENCES

[1] 刘振亚. 中国电力与能源[M]. 北京：中国电力出版社，2012：124-135.
Liu Zhenya. Electric power and energy in China [M]. China Electric Power Press，2012：124-135(in Chinese).

[2] Zheng Jie，Mehndiratta S，Guo J Y，et al. Strategic policies and demonstration program of electric vehicle in China [J]. Transport Policy，2012，19(1)：17-25.

[3] Venayagamoorthy G K. Smart charging stations for short term power flow control in smart grids[C]//IEEE International Electric Vehicle Conference(IEVC) 2012. Greenville，USA：IEEE，2012：1-6.

[4] Mitra P，Venayagamoorthy G K. Smart charging station as a virtual STATCOM[J]. IEEE Transactions on Smart Grid，2011，2(3)：445-455.

[5] Mitra P，Venayagamoorthy G K. Intelligent coordinated control of a wind farm and distributed smart charging stations[C]//IEEE Industry Application Society Annual Meeting(IAS) 2010. Houston，USA：IEEE，2010：1-8.

[6] Tomic J，Kempton W. Using fleets of electric drive vehicles for grid support[J]. Journal of Power Sources，2007，168(2)：459-468.

[7] Kempton W，Tomic J. Vehicle-to-grid power fundamentals：calculating capacity and net revenue [J]. Journal of Power Sources，2005，144(1)：268-279.

[8] 王锡凡，邵成成，王秀丽，等. 电动汽车充电负荷与调度控制策略综述[J]. 中国电机工程学报，2013，33(1)：1-10.
Wang Xifan，Shao Chengcheng，Wang Xiuli，et al. Survey of electric vehicle charging load and dispatch control strategy[J]. Proceedings of the CSEE，2013，33(1)：1-10(in Chinese).

[9] Kempton W，Tomic J. Vehicle-to-grid power implementation：from stabilizing the grid to support large-scale renewable energy[J]. Journal of Power Sources，2005，144(1)：280-294.

[10] 田立亭，张明霞，汪奂伶. 电动汽车对电网影响的评估和解决方案[J]. 中国电机工程学报，2012，V32(31)：43-49.
Tian Liting，Zhang Mingxia，Wang Huanling. Evaluation and solutions for electric vehicles' impact on the grid [J]. Proceedings of the CSEE，2012，32(31)：43-49(in Chinese).

[11] Huston C，Venayagamoorthy G K，Corzine K. Intelligent scheduling of hybrid and electric vehicle storage capacity in a parking lot for profit maximization in grid power transaction[C]//Proceedings of IEEE Energy 2030. Atlanta，USA：IEEE，2008：1-8.

[12] 李正烁，孙宏斌，郭庆来，等. 计及碳排放的输电网侧“风-车协调”研究[J]. 中国电机工程学报，2012，32(10)：41-48.
Li Zhengshuo，Sun Hongbin，Guo Qinglai，et al. Study on wind-EV complementation on the transmission grid side considering carbon emission[J]. Proceedings of the CSEE，2012，32(10)：41-48(in Chinese).

[13] Beck L J. V2G – 101，a text about vehicle-to-grid(V2G)，the technology which enables a future of clean and efficient electric-powered transportation[M]. USA：V2G-101 Copyright，2009：10-25.

[14] Yu Yaonan. Electric power system dynamics[M]. New York：Academic Press，1983：79-94.

[15] 杜文娟，王海风，曹军. PSS 就地相位补偿法的模型和理论[J]. 中国电机工程学报，2012，32(19)：36-41.
Du Wenjuan，Wang Haifeng，Cao Jun. Model and theory of PSS localized phase compensation method [J]. Proceedings of the CSEE，2012，32(19)：36-41(in Chinese).

[16] 杜文娟，王海风，曹军. 稳定器设计的就地相位补偿法在多机电力系统中的应用[J]. 中国电机工程学报，2012，32(22)：73-78.
Du Wenjuan，Wang Haifeng，Cao Jun. Application of localized phase compensation method to design a stabilizer in a multi-machine power system [J]. Proceedings of the CSEE，2012，32(22)：73-78(in Chinese).

[17] Du Wenjuan，Wang Haifeng，Xiao Liye. Power system

small- signal stability as affected by grid-connected photovoltaic generation[J]. European Transactions on Electrical Power，2012，22(5)：688-703.

[18] Du Wenjuan，Wang Haifeng，Cai Hui. Modeling a Grid-connected SOFC power plant into power systems for small-signal analysis and control[J]. European Transaction on Electrical Power，2012，23(3)：330-341.

[19] Wang Haifeng，Swift F J. The capability of the static var compensator in damping power system oscillations [J]. IEE Proceedings of Generation，Transmission and Distribution，1996，143(4)：353-358.

[20] Majeau-Bettez G，Hawkins T R，Stroemman A H. Life-cycle environmental assessment of lithium-ion and nickel metal hydride batteries for plug-in hybrid and battery electric vehicles[J] . Environmental Science and Technology，2011，45(10)：4548-4554.

[21] Stikes K，Gross T，Zhao Lin，et al. Plug-in hybrid electric vehicle market introduction study ： final report [R]. Washington，DC：Tech. Rep. DE2010-972306，2010.

[22] Hu Guoqiang，He Renmu，Yang Huachun，et al. Iterative prony method based power system low frequency oscillation mode analysis and PSS design[C]//2005 IEEE/PES Asia and Pacific Transmission and Distribution Conference and Exhibition. Dalian，China：IEEE，2005：1-6.

Appendix　A　The parameters of example systems

1）Single-machine infinite-busbar power system.

The parameters of the synchronous machine (the unit is in pu):

M=5.0 ； T'_{d0}=5.0 s ； D=1.2 ； X_d=0.8 ； X_q=0.4 ； X'_d=0.05 ； ω_0=2×50π ; U_t=1.05 ; U_{tref}=1.05 ; K_a=20.0 ; T_a=0.01 s .

The parameters of the network (The unit is in pu)：X_{ts}=0.2 ; X_{sb}=0.1 ; X_s=0.1 ; U_b=1.0 .

The parameters for the smart charging station(The unit is in pu)：K_{PP}=20, K_{IP}=20, K_{PI_q}=0.3, K_{II_q}=0.3 ， K_{PQ}=15, K_{IQ}=15, K_{PI_d}=0.7, K_{II_d}=0.7 .

2）Four-machine power system.

The parameters of the synchronous machine are：T_{J1}=T_{J2}=117 ； T_{J3}=T_{J4}=111.15 ； T'_{d01}=T'_{d02}=T'_{d03}=T'_{d04}=8.0 s ； D_{mac1}=D_{mac2}=D_{mac3}=D_{mac4}=5.0 pu ； X_{d1}=X_{d2}=X_{d3}=X_{d4}=0.2 ； X_{q1}=X_{q2}=X_{q3}=X_{q4}=0.1889 ； X'_{d1}=X'_{d2}=X'_{d3}=X'_{d4}=0.0333 ； ω_{01}=ω_{02}=ω_{03}=ω_{04}=100π ； U_{t1}=U_{t3}=1.03 ； U_{t2}=U_{t4}=1.01 ； U_{tref1}=U_{tref3}=1.03 ; U_{tref2}=U_{tref4}=1.01 .

All the generators are equipped with the same AVR. K_a=50; T_a=0.55s.

The parameters of the smart charging station are (in pu): K_{PP}=20, K_{IP}=20, K_{PI_q}=0.3, K_{II_q}=0.3 ; K_{PQ}=15, K_{IQ}=15, K_{PI_d}=0.7, K_{II_d}=0.7 .

The parameters of the lines are (in pu): X_{15}=X_{36}=X_{29}=X_{48}=0.01667 ； X_{56}=X_{89}=0.025 ； X_{67}=0.105; X_{78}=0.005 .

G1 is connected with the slack bus of the system. G3 and G4 generate 70 MW active power respectively. The loads at Bus 6 and Bus 8 are 100 MW and 200 MW accordingly.

收稿日期：2013-07-01。

蔡晖

作者简介：

蔡晖(1984)，男，博士，主要从事电网规划、新能源接入电网后对电网影响及电动汽车充放电策略等方面的研究，caihui300@hotmail.com；

黄俊辉(1965)，男，高级工程师，从事电网规划研究及管理工作，huangjh@js.sgcc.com.cn；

王海潜(1963)，男，高级工程师，从事电力系统规划研究工作，15951900696@139.com；

谢珍建(1980)，男，高级工程师，从事电网规划与管理工作，zhenjianxie@163.com；

陈麒宇(1986)，男，博士研究生，研究方向为新能源接入下的电力系统运行与控制，Qchen05@qub.ac.uk；

Tim LITTLER，男，博士，博士生导师，研究方向包括电力系统、风机及新能源的接入、智能电网、电力系统分析、保护及稳定、数据可靠性及方法的研究及优化方法的研究，t.littler@ee.qub.ac.uk。

(责任编辑　刘浩芳)

特约主编寄语

主动配电网是以公共配电网（可有条件孤岛运行）的方式，而微网是从专网（可无条件孤岛运行）的方式处理接入的分布式资源（分布式发电、可再生能源、交互式负荷、电动汽车、储能），主动配电网与微网都是提高可再生能源渗透率与平滑负荷（削峰）的成本效益较高的技术手段，同属智能配电网研究的范畴。《中国电机工程学报》针对国内外这一智能配电网研究的热点问题，设定了“主动配电网和微网技术研究”专栏，本人非常荣幸地受邀担任此次特别策划专栏的特约主编。鉴于主动配电网的研究还处于启动阶段，本专栏一是将持续刊出所录用的论文，二是希望专家学者能够在这个专栏继续发表最新研究成果。作为特约主编，希望借此机会，与相关的专家学者共同比较国内外配电网发展的差异，从而思考我国研究智能配电网应该关注的主要问题，以期对未来的深入研究有所帮助。

我国的智能配电网建设需要兼顾智能化和配电网扩容发展的问题。我国配电网自动化程度较低，配电信息化系统也还处于布署阶段，配电网络大都仍处于不可观、不可测和不可控的状态，其控制方式和管理模式到目前为止主要采用的是被动的模式。此外，我国现有的配电网资产平均年限较短（如 10~20 年），不宜进行大规模更新改造，而负荷仍以每年 7%的速度增长，配电网络还以相应的规模在扩大，当前建设的配电网络可能未来 50 年仍有可能在使用，因此，我国不仅要研究通过主动控制和主动管理达到平滑负荷需求与提高可再生能源渗透率（可再生能源发电量占总用电量的比例）的问题，还要研究现有配电网的充分利用和扩展的问题。

国外经济发达国家智能配电网建设主要注重智能化问题。因为经济发达国家配电网的负荷发展已基本饱和，配电网自动化程度较高、信息化集成度高，其智能电网研究关注的主要重点是智能化问题（通讯、信息化、控制和电力电子技术等），较少在讨论智能化时还探讨配电网本身的扩展模式。由于配电网络运行年限相对较长，部分供电区域已经到了更新换代的阶段，故可从网络整体更新考虑网络扩展问题，如网状网络、直流配电或交直流混合配电技术以及提高配电电压等级等。因此，发达国家研究在一个时间周期内对分布式资源进行主动控制和主动管理，以达到平滑负荷（削峰）及提高可再生能源渗透率的目的，这有赖于比传统信息在集成度和准实时性要高几个数量级的信息，传统分散型的企业信息系统往往难以胜任。

此次专题征稿得到了国内外专家学者的大力支持，共约提交了 120 余篇论文。经各位特约评审专家认真评审，共录用了 30 余篇。本期专栏汇总了 9 篇论文，多角度地深入讨论解决中国微网和主动配电网的适用可行技术，应该强调的是，论文一是要探讨解决具体的技术方案、二是要探讨其成本效益和推广应用价值。

中国电力科学研究院 范明天，2014-06-05